A Multi-Objective Optimization Approach to Coverage Path Planning of Agricultural Drone

Fabian Andres Lara-Molina, Fran Sérgio Lobato, and Maicon Fábio Appelt

***Abstract*—Agricultural drones have been widely used in precision agriculture operations due to their high performance and adaptability to outdoor tasks, such as spraying, mapping, and monitoring. Nevertheless, mission planning remains challenging due to the constraints imposed by operational performance under real field conditions. In this work, a novel multi-objective optimization approach for mission planning of agricultural spraying drones is proposed. This approach contemplated an off-line coverage path planning strategy that simultaneously minimizes total mission time and energy consumption. The parameters that define the coverage path are optimized while considering the operational requirements of the spraying tasks. The framework is applied to a real case study using the DJI AGRAS T10 drone in a crop field. The results obtained from the multi-objective optimization demonstrate significant performance gains in terms of reduction in battery energy consumption of up to 14.2% and a mission time decrease of 9.5% when compared to conventional geometric methods. Thus, the proposed method potentially reduces both the drag energy and the mission time. These findings highlight the potential of multi-objective optimization as a decision-support tool to improve the efficiency and sustainability of drone-based spraying operations in agriculture.**

Link to graphical and video abstracts, and to code:
https://latamt.ieeer9.org/index.php/transactions/article/view/10298

***Index Terms*—Precision agriculture, agricultural drones, multi-objective optimization, coverage path planning.**

NOMENCLATURE

A	Reference area of the drone
C_D	Drag coefficient
E	Energy
f	Objective functions
h	Drone altitude
L_t	Sweep lines
P_{Drag}	Drag power
$\mathbf{p}_H$	Home position
T	Total number of parallel sweep lines
t_a	Battery endurance
v	Drone velocity
x_d, y_d	Position coordinate
δ_r	Row spacing
θ	Sweep direction
$\boldsymbol{\lambda}$	Design variables
ρ	Air density
ω	Drone angular velocity
$\mathfrak{M}$	Target area

The associate editor coordinating the review of this manuscript and approving it for publication was Guillermo Valencia-Palomo (*Corresponding author: Fabian Andres Lara Molina*).

Fabian Andres Lara Molina is with the Department of Mechanical Engineering, Federal University of Triângulo Mineiro, Uberaba-MG, Brazil (e-mail:fabian.molina@uftm.edu.br).

F. S. Lobato is with the School of Chemical Engineering, Federal University of Uberlândia, Uberlândia-MG, Brazil (e-mail:fslobato@ufu.br).

M. F. Appelt is a Research Engineer with Fertirriga, Rio Paranaíba-MG, Brazil (e-mail:maicon@fertirriga.com.br).

I. INTRODUCTION

TECHNOLOGIES once confined to industrial manufacturing, such as robotics and automation, are now gaining traction in agriculture to support sustainable food and energy production. Specifically, robotics and automation have emerged as technologies that permitted dealing with the dual pressures of decreasing arable land and a rapidly expanding global population. In this regard, increasing crop productivity is a demanding imperative that is constrained by environmental impacts, land use limitations, and the prevalence of plant diseases. In this context, Artificial Intelligence (AI) and the Internet of Things (IoT) have proven to be transformative, offering new opportunities for optimizing agricultural practices [1]. Recent studies highlight the integration of AI and IoT as a means to increase the efficiency and sustainability of agricultural systems [2]. Despite their broad adoption and many potential benefits, agricultural drones continue to encounter technical and operational limitations that need to be addressed to unlock their full potential and foster further progress in the field. Even so, their integration has already brought substantial improvements to precision agriculture, particularly in applications such as crop mapping, real-time monitoring, automated spraying, and yield forecasting [3].

Unmanned Aerial Vehicles (UAVs), a specialized category of agricultural drones, are developed to perform tasks such as crop surveillance, aerial spraying, field mapping, seeding, and identifying weeds or pests [4]. They are generally outfitted with advanced technologies and sensors widely applied in precision agriculture, such as Real-Time Kinematic (RTK) Global Positioning System, multispectral imaging systems, temperature sensors, as well as liquid reservoirs and spraying mechanisms. Through the acquisition and processing of real-time data, these drones enable better resource utilization, increase operational efficiency, and contribute to improved crop health and productivity [5]. Coverage Path Planning (CPP) refers to the process of generating trajectories that allow a drone to systematically and efficiently cover a specified area. A significant emphasis in CPP research lies in flight path optimization, with key goals including reducing energy consumption and minimizing overall mission duration [6], [7]. Several studies have investigated the core principles and techniques applied in this domain [8]. To be effective, CPP strategies must also incorporate the dynamic constraints

associated with drone motion. A variety of studies have investigated methods to optimize drone coverage paths. For instance, Bostelmann-Arp *et al.* [9] proposed a multi-objective seed curve optimization approach for coverage path planning in precision farming, considering three objectives: coverage, energy efficiency, and path precision, defined by the angle relative to the flight direction. Similarly, Tian *et al.* [10] developed and validated a multi-objective waypoint planning algorithm for UAV spraying based on the ant colony algorithm, which proved effective in reducing flight energy consumption. In another study, Ellefsen *et al.* [11] applied evolutionary multi-objective optimization to inspection path planning, leveraging evolutionary search to identify energy-efficient inspection trajectories. Multi-objective optimization has also been applied to coverage path planning of quadcopter swarms, enabling path optimization without imposing shape constraints [12]. Furthermore, Ellefsen *et al.* [13] addressed multi-objective CPP for complex 3D structures, simultaneously improving inspection coverage and reducing energy consumption.

Recent path planning research has explored bio-inspired strategies and hybrid learning methods, such as membrane-based potential fields and Q-learning algorithms, to improve navigation in complex or unknown spaces [14], [15], [16]. While these methods are highly effective for point-to-point obstacle avoidance, the approach proposed in the present contribution addresses the systematic CPP problem, which focuses specifically on the unique trade-offs between spray overlap and energy consumption required for agricultural aerial applications.

Several research works have addressed the UAV path planning problem by applying multi-objective optimization approaches, as methods proposed for path planning often fail to handle conflicting goals effectively, resulting in unsatisfactory paths. A multi-objective evolutionary algorithm based on dimensional exploration and discrepancy evolution is presented to identify key dimensions to facilitate prior exploration [17] effectively identified key dimensions for exploration, resulting in more robust trajectory sets. A multi-objective optimization approach was proposed to monitor traffic situations and optimize the respective cruise route [18] reducing cruise route costs while maintaining high coverage rates. A multi-objective particle swarm optimization algorithm was proposed for the multi-UAV path planning problem in a complex three-dimensional environment [19] achieving superior convergence and collision-free paths. A multi-objective path planning framework for urban environments was developed, focusing on minimizing journey distance and enhancing safety level [20], successfully minimizing journey lengths while enhancing safety by avoiding high-risk zones. A path-planning approach for UAVs in known, static, rough terrain yielded feasible paths with minimal altitude variation [21]. A multi-UAV cooperative trajectory planning model was proposed to convert the problem into a many-objective optimization problem [22], minimizing coordination costs and threat exposure. A multi-objective NSGA-II optimization was employed to plan flight trajectories, aiming to minimize energy consumption while maximizing the average received signal strength indicator [23], achieving improvements of up to 70.25% in average signal strength. The previous works mainly use multi-optimization to plan UAV's paths for exploration missions; nevertheless, the CPP of agricultural drones and its main limitation imposed by the battery endurance have not been addressed yet.

Although previous studies have proposed multi-objective strategies for coverage path planning, addressing aspects such as coverage efficiency, energy consumption, waypoint optimization, and inspection of complex structures, most existing approaches either focus on generic UAV operations or consider only a limited subset of mission parameters. In particular, few works explicitly integrate the operational requirements of agricultural spraying missions, where factors such as row spacing, sweep direction, and drone velocity directly influence both energy efficiency and mission duration. This gap underscores the need for a comprehensive mission planning framework specifically designed for agricultural spraying drones, which can simultaneously minimize energy consumption and mission time under realistic operational conditions. In this study, a multi-objective optimization framework for mission planning of agricultural spraying drones was developed. The proposed approach formulates an off-line coverage path planning strategy that simultaneously minimizes mission time and energy consumption. Consequiently, operational parameters such as row spacing, sweep direction, and drone velocity are optimized under realistic spraying conditions to provide a comprehensive approach that enhance the efficiency and performance of drone-based agricultural operations.

There is a gap regarding the simultaneous optimization of energy and time for coverage paths applied to agricultural fields despite the development of path planning approaches. Most existing methods do not account for the varying power demands of different sweep angles and row spacings. The first contribution of the proposed approach consists of the development of a multi-objective optimization framework for CPP, which considers not only the geometric description of the target area but also the dynamic efficiency challenge. By providing a set of Pareto-optimal solutions, this approach allows operators to select missions based on real-time priorities (e.g., speed vs. battery longevity). Moreover, this case study evaluates the performance of some meta-heuristics (NSGA-II, MOEA/D (Multi-Objective Evolutionary Algorithm based on Decomposition [24]), and SPEA2 (Strength Pareto Evolutionary Algorithm 2 [25])) applied to the operational parameters of a DJI AGRAS T10 (Fig. 1a), a commercial agricultural UAV designed for precision spraying and equipped with RTK-based positioning and automated flight control systems, enabling the establishment of a new baseline for autonomous mission planning.

The study presented in this manuscript proposes a novel approach for optimizing the mission planning of agricultural spraying drones using a multi-objective optimization framework. The approach consists of designing an off-line coverage path planning with the following key contributions:

1) A Multi-Objective Framework: a comprehensive mission-planning framework was proposed to optimize drone-based agricultural spraying by balancing concurrent objectives (mission time and power consumption).

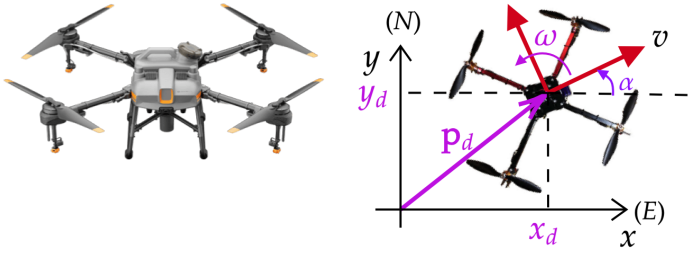

(a) DJI AGRAS T10 Sprayer Drone [26].

(b) Drone configurations

Fig. 1. Operational and geometric definitions of the sprayer drone: the sweep direction (θ), row spacing (ω), and drone position ($\mathbf{p}_d$).

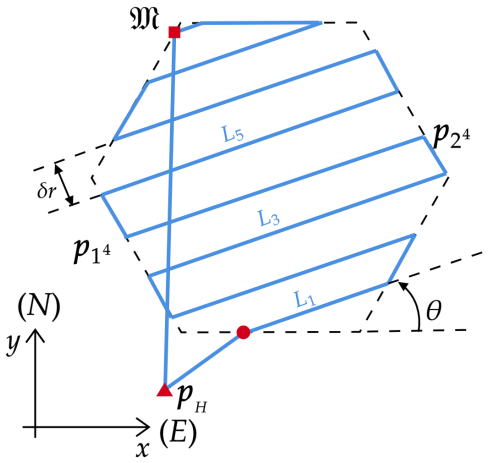

Fig. 2. Geometric representation of the CPP for a convex polygon. The blue lines indicate the flight trajectories calculated to ensure overlap consistency and mission efficiency.

2) Integrated Path and Parameter Optimization: geometric path variables (e.g., row spacing and sweep direction) and kinematic parameters (e.g., drone velocity) are simultaneously optimized within a single decision-making loop, unlike traditional methods.
3) Efficiency-Driven Mission Planning: an optimization strategy that treats mission time and energy consumption as dynamic objective functions, allowing for realistic mission planning that adapts to specific field geometries and drone constraints.

The paper is organized into four primary sections. The section material and methods present the multi-objective optimization approach applied to the coverage path. The section results and discussions report and analyze the numerical findings from the optimization process. Finally, the main conclusions of the work highlight potential avenues for future research.

II. Material and Methods

An agricultural spraying operation utilizes drones to distribute agrochemicals, including herbicides, pesticides, and fertilizers, across crop areas. The present approach aims to plan optimally for a spraying operation using an agricultural drone based on a multi-objective optimization approach.

A. Drone Definitions

For the present study, the state vector $\mathbf{q} = (\mathbf{p}_d, \alpha)$ defines the drone configuration with $\mathbf{p}_d = (x_d, y_d, z_d)$ representing the position coordinates in the north-east-down (NED) reference frame, and α being the angle relative to the east axis (Fig. 1b). Moreover, ω and v represents the drone's angular velocity (i.e., yaw rate) and its translational velocity along a linear trajectory, respectively.

In typical spraying missions, the target area to be covered by the drone can be effectively represented by a convex polygon. Accordingly, two main assumptions are taken into account in the target area modeling: i) A small set of vertices is used to delineate the area, and ii) there are no obstacles exceeding a predefined height within the region [6]. Considering these assumptions, a convex polygon $\mathfrak{M}$ with n_v vertices $\mathbf{v}_i$ ($i = 1, \ldots, n_v$) is considered to model the target area. Therefore, $\mathfrak{M} = \mathbf{v}_1, \mathbf{v}_2, \ldots, \mathbf{v}n_v$, where each vertex $\mathbf{v}_i = (x_i, y_i) \in \mathbb{R}^2$ for $i = 1, \ldots, n_v$.

B. Coverage Path

The operational settings of Fig. 2 that define the coverage path are: sweep angle (θ) of the coverage lines, row spacing (δ_r), home position (p_H), and battery endurance (t_a). The definition of different sweep angles (θ) and row spacing (δ_r) vary the number of turns and path lengths depending on the geometry of the polygon. The selection of the sweep direction, row spacing, and drone velocity becomes essential to minimize the overall coverage time (see Fig. 2).

For the present study, the design variables that define the coverage path are the parameters that can be imposed in the control of the drone to execute a determined flight mission [26]. These design variables are set in the vector $\boldsymbol{\lambda} = [\delta_r \quad \theta \quad v]^T$ with v being the linear velocity of the drone, and its angular velocity (ω) is fixed at a specific value. The row spacing δ_r is defined by the manufacturer's effective spray width to ensure the trajectories maintain 100% coverage of the target area.

Therefore, the following conditions are considered in the definition of the coverage path:

- A convex polygonal region $\mathfrak{M} \subset \mathbb{R}^2$
- A fixed number T of parallel sweep lines $\{L_1, L_2, \ldots, L_T\}$
- A home/refueling station at position $\mathbf{p}_H \in \mathbb{R}^2$
- A coverage footprint width δ_r, determining spacing between sweep lines
- A maximum flight time (fuel constraint) t_a

The angle of the sweep lines (concerning the x-axis), denoted by θ, determines the orientation of all coverage lines L_t and, consequently, the corresponding set of waypoints.

Each sweep line $L_t(\theta)$ of intersects the polygon and is discretized into two waypoints that intercept the polygon:

$$L_t(\theta) = \{\mathbf{p}_{1^t}, \mathbf{p}_{2^t}\}, \quad \text{for } t = 1, \ldots, T, \tag{1}$$

each waypoint $\mathbf{p}_{i^t} \in \mathbb{R}^2$ for $i = 1, 2$ is inside the polygon. Equation (1) represents the set of coordinates of a sweep line for a given sweep direction θ.

C. Objective Functions

1) Mission Time: The mission time (coverage time) is denoted by $c(\boldsymbol{\lambda})$ and it is formulated as a function of the design variables $\boldsymbol{\lambda} = [\delta_r \quad \theta \quad v]^T$. The total time required by the drone to traverse all waypoints, as expressed in

$$c(\boldsymbol{\lambda}) = \sum_{t=1}^{T} c(\mathbf{p}_{i^t}, \mathbf{p}_{i+1^t}), \tag{2}$$

the expression of Equation (2) is used to evaluate the path execution time.

The waypoints' location over the borders of the target area will depend on the sweep angle (θ) and row spacing (δ_r). Thus, considering $\mathbf{p}_{i^t}$ and $\mathbf{p}_{i+1^t}$ as two consecutive waypoints along the t-th coverage line for $t = 1, \ldots, T$ (see Fig. 2). The time required for the drone to reorient and travel between these two waypoints is defined by the cost function:

$$c(\mathbf{p}_{i^t}, \mathbf{p}_{i+1^t}) = \frac{\theta_\Delta}{\omega} + \frac{\|\mathbf{p}_{i+1^t} - \mathbf{p}_{i^t}\|}{v}, \tag{3}$$

where θ_Δ represents the change in heading angle between the segments, v is the drone's linear velocity, and ω is its angular velocity. The cost function of Equation (3) is required to compute the total time of Equation (2).

2) Energy Consumption: In addition to hovering and elevation, the energy consumed during horizontal motion of the drone is significantly affected by aerodynamic drag. In the present study, drag energy is considered, as the drone's coverage motion is restricted to the xy plane. Following the framework presented by Thibbotuwawa *et al.* [27], the total energy consumption can be expressed as the sum of two components of the energy consumed $E(\boldsymbol{\lambda})$:

$$E(\boldsymbol{\lambda}) = E_{Hover} + E_{Drag}. \tag{4}$$

The drag power, originated from the drag energy of Equation (4), is consider since the drone motion is confined over the $x - y$ plane that is the motion carry out in the coverage path at a fixed altitude. Thus, the drag power is defined as:

$$p_{Drag}(\boldsymbol{\lambda}) = \frac{1}{2}\,\rho\, v^3\, C_D\, A, \tag{5}$$

where ρ is the air density, v is the flight velocity, C_D is the drag coefficient, and A is the reference area of the drone

This relationship shows that drag power increases with the cube of velocity, highlighting the strong impact of flight speed on energy efficiency. The corresponding drag energy is obtained by multiplying the drag power of Equation (5) by the flight duration $c(\boldsymbol{\lambda})$ according to:

$$E_{Drag}(\boldsymbol{\lambda}) = p_{Drag}\, c(\boldsymbol{\lambda}). \tag{6}$$

The formulation of Equation (6) enables quantifying the contribution of aerodynamic drag to the overall energy consumption, which is particularly relevant for mission planning and trajectory optimization of drones.

D. Multi-Objective Optimization

The multi-objective optimization aims to determine the optimal design variables of the coverage path to improve drone performance. These design variables include row spacing (δ_r), sweep direction (θ), and drone velocity (v). As illustrated previously, performance was defined in terms of mission time (see Equation (2)) and energy consumption (see Equation (6)). Consequently, the criteria presented in the last section are used as objective functions in the multi-objective optimization.

The design variables are defined as the vector $\boldsymbol{\lambda} = [\delta_r \quad \theta \quad v]^T$. Hence, the multi-objective optimization consists of minimizing the mission time and simultaneously minimizing the energy consumption due to the horizontal movement. These two objectives are concurrent because the minimization of mission time implies an increase in the drone's velocity (v), which also increases the energy consumption that is proportional to the velocity, according to the definition of the objective functions. Therefore, this optimal design procedure results in a multi-objective optimization problem, where multiple objectives must be optimized simultaneously, as shown in:

$$\min_{\boldsymbol{\lambda}} \{f_1 = c(\boldsymbol{\lambda}), f_2 = E_{Drag}(\boldsymbol{\lambda})\} \tag{7}$$

Subject to

$$\begin{aligned} &\underline{\delta}_r < \lambda_1 < \overline{\delta}_r \\ &\underline{\theta} < \lambda_2 < \overline{\theta} \\ &\underline{v} \leq \lambda_3 \leq \overline{v}. \end{aligned} \tag{8}$$

NSGA-II is employed to solve this multi-objective optimization problem, as it is widely recognized for its efficiency in handling complex, nonlinear problems with conflicting objectives and for providing a well-distributed set of Pareto-optimal solutions. This algorithm has been successfully applied to a wide range of engineering design problems, including the geometric optimization of robotic manipulators [28], [29] and the design of robust engineering systems [30].

Finally, the algorithm to compute the coverage path is presented in the flow chart of Fig. 3. The optimization of the coverage path is computed based on the NSGA-II algorithm to a set of optimal solutions denominated Pareto front [31]. Initially, a set of candidate solutions. The objective functions, namely mission time and energy consumption, are evaluated for these candidate solutions to generate the Pareto front until the stopping criteria are met after the iterative application of genetic algorithm operations (crossover and mutation).

The effectiveness of the optimization objectives and constraints must be validated across diverse scenarios. The following section presents the numerical results to distinct field geometries.

III. Results and Discussion

The present application considers the DJI AGRAS T10 drone. Accordingly, the following fixed parameters were adopted for the case study to optimize mission planning based on the proposed method described in Sec. II. Moreover, the maximum angular velocity $\omega = 45°$/s, and autonomy time per sortie $t_a = 560$ s (8 minutes). For the energy consumption,

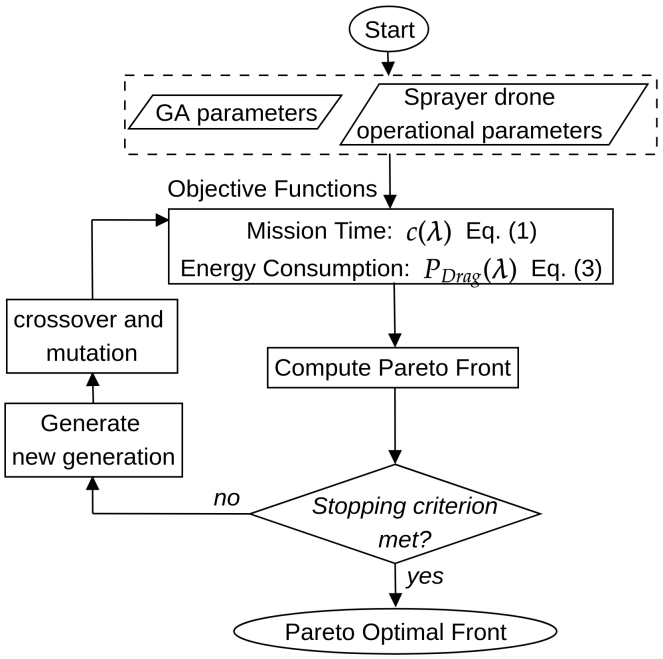

Fig. 3. Flowchart of the multi-objective coverage path optimization.

the following parameters were selected for the DJI AGRAS T10, ρ= 1.2 kg/m^3 and C_DA= 0,20 m^2 [26]. The proposed algorithm was implemented in Python, and all numerical simulations were performed on a system running Ubuntu 20.04 with an Intel Core i7 processor.

This section considers the solution of the multi-objective optimization problem of Eq. (7) in section II. For the numerical results presented in this section, the multi-objective optimization problem was solved using the NSGA-II, MOEA/D and SPEA2 algorithms implemented in the *pymoo* library.

The multi-objective optimization problem was solved using three different meta-heuristics algorithms: NSGA-II, MOEA/D, and SPEA2. These algorithms were configured with a uniform population of 100 individuals and evolved over 100 generations to ensure a fair comparison of computational effort and convergence performance. The search space was explored using the Simulated Binary Crossover operator with a probability of 0.9 and a distribution index of 15. In contrast, a Polynomial Mutation operator with a distribution index of 20 was employed to maintain population variability. For NSGA-II and SPEA2, duplicate solutions were strictly eliminated to preserve diversity. The resulting Pareto-optimal solutions were sorted according to the first objective function (Mission Time) to facilitate interpretation. These hyperparameter settings were finalized after preliminary runs demonstrated stable convergence across all investigated field geometries, providing a robust baseline for the comparative analysis.

The design variables are constrained according the following definitions (as presented in Eq. (8)): coverage footprint spacing $\underline{\delta}_r$ = 4.5 m and $\overline{\delta}_r$ = 6.5 m; sweep angle $\underline{\theta}$=0 ° and $\overline{\theta}$ =360 °; and velocity $\underline{v}$ = 6 m/s and $\overline{v}$ = 8 m/s.

TABLE I
DESIGN VARIABLES ($\boldsymbol{\lambda}_i$) AND OBJECTIVES FUNCTIONS (f_1, f_2) OF THE PARETO FRONT (FIG. 5A) FOR THE POLYGON 1 (FIG. 4A)

$\boldsymbol{\lambda}_i$	δ_r	θ	v	f_1	f_2
1	6.4999	44.3079	7.9999	308.9658	5.2730
2	6.4998	44.2634	7.7766	316.8337	4.9668
3	6.4999	44.3155	7.5838	323.9372	4.7099
4	6.4999	44.3269	7.3482	333.1637	4.4064
5	6.4999	44.2718	7.1086	343.2134	4.1097
6	6.4999	44.2606	6.9496	350.2521	3.9187
7	6.4999	44.3072	6.7387	360.0538	3.6726
8	6.4999	44.2504	6.5138	371.2831	3.4205
9	6.4999	44.3068	6.3635	379.1593	3.2568
10	6.4999	44.3153	6.1454	391.3295	3.0275

A. Numerical Examples

For this section, four distinct convex polygons were considered, including shapes with varying complexity: a nonagon (nine vertices, Fig. 4a), a pentagon (five vertices, Fig. 4b), a rectangle (four vertices, Fig. 4c) and a 36-sided regular polygon (polygonal approximation of a circle in Fig. 4d).

The optimal solutions of the obtained Pareto front are compared to the approaches proposed by Choset and Pignon [32] and Torres *et al.* [33] (see Appendix A) that permit obtaining the sweep direction (θ). Moreover, the middle values (according to Eq. (8)) for the row spacing (δ_r) and the drone velocity (v) were considered to compute the coverage paths and thus establish a fair comparison.

1) Polygon 1: The Pareto front, considering the target area defined by a polygon with nine vertices, is present in Fig. 5a. One can observe that minimizing the mission time $c(\boldsymbol{\lambda})$ implies maximizing the drag energy. This behavior occurs due to the influence of the drone's velocity; the higher the drone's velocity, the shorter the mission time ($c(\boldsymbol{\lambda})$). However, at the same time, it increases the drag energy required for the horizontal drone motion ($E_{Drag}(\boldsymbol{\lambda})$).

The results obtained for the coverage paths using the approaches proposed by Choset and Pignon [32] and Torres *et al.* [33] are also present in Fig. 5a. These results are non-dominant, i.e., they do not minimize the mission time nor the drag energy when compared to the results obtained on the Pareto front. The baseline methods of Choset [32] and Torres *et al.* [33] were selected for comparison as they represent the foundational geometric methods still widely utilized in commercial agricultural UAV software. This comparison is crucial for demonstrating the performance of the proposed multi-objective approach gains over established industry standards.

The definition of the ten selected solutions of the Pareto-front (F_i for $i = 1, \ldots, 10$) is defined in Table I. Moreover, the corresponding design variables that specify the definition of the coverage path are also defined in table I ($\boldsymbol{\lambda} = [\delta_r \quad \theta \quad v]^T$ for $i = 1, \ldots, 10$). The optimal solutions illustrated in table I indicate that row spacing (δ_r) attains its maximum value for all solutions to minimize the path distance and consequently the mission time and drone energy. Moreover, the obtained sweep angle (θ) was optimally adjusted to minimize the path distance.

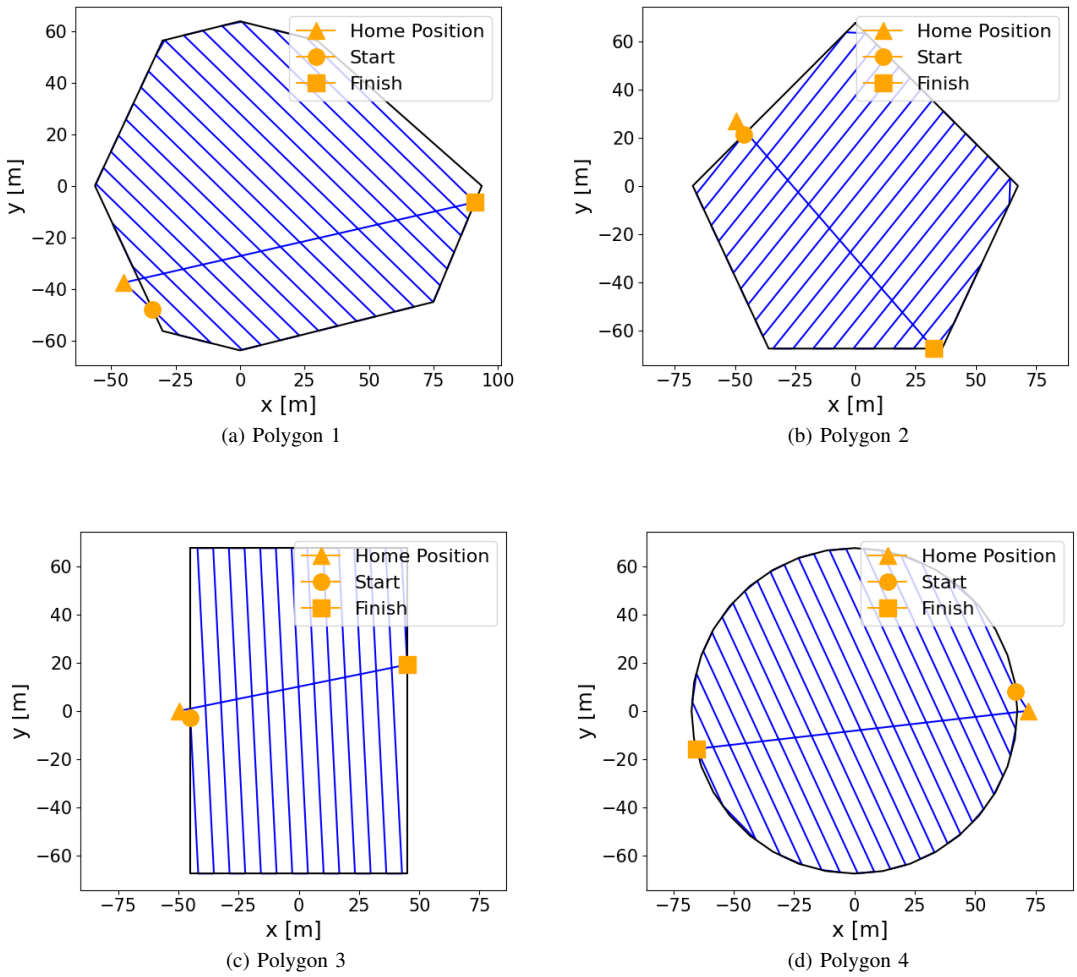

(a) Polygon 1 (b) Polygon 2

(c) Polygon 3 (d) Polygon 4

Fig. 4. Convex polygons considered as target area in the spraying mission and coverage path from the multi-objective optimization corresponding to $\boldsymbol{\lambda}_6$.

Finally, the coverage path (PC) over the target area is presented in Fig. 4a, considering the sixth optimal solution of Table-I and the solution using the approach according to Torres *et al.* [33] (see Fig. 5a). The coverage path obtained with the multi-objective method (Fig. 4a) requires a shorter distance from the home position to initiate the coverage path, which minimizes both energy consumption and mission time.

2) Polygon 2: One can observe an equivalent output behavior for the second target area obtained from the previous case study. The Pareto-front for this case study is presented in Fig. 5b. One can observe that these two objectives are also concurrent for this case study. Moreover, the obtained mission time follows the maximum endurance of the battery $c(\boldsymbol{\lambda} < t_a)$.

Table II shows the design parameters $\boldsymbol{\lambda}$ that define the coverage paths of the Pareto-front of Fig. 5b. The results permit the evaluation of the specific solution $\boldsymbol{\lambda}_i$ for $i = 1, \ldots, 10$ that could be implemented to obtain a determined output of the coverage path. On the one hand, the optimal solution F_1 considers the shorter mission time. Nevertheless, it requires more drag energy. On the other hand, the optimal solution F_{10} prioritizes energy consumption over mission time.

TABLE II
DESIGN VARIABLES ($\boldsymbol{\lambda}_i$) AND OBJECTIVES FUNCTIONS (f_1, f_2) OF THE PARETO FRONT (FIG. 5B) FOR THE POLYGON 2 (FIG. 4B)

$\boldsymbol{\lambda}_i$	δ_r	θ	v	f_1	f_2
1	6.4999	128.7438	7.9998	279.6485	4.7724
2	6.4999	128.7448	7.8333	284.8112	4.5633
3	6.4999	128.7490	7.6220	291.6887	4.3054
4	6.4999	128.7447	7.4046	299.1740	4.0487
5	6.4879	128.7647	7.1734	308.0088	3.7899
6	6.4999	128.7823	6.9677	315.6381	3.5591
7	6.4999	128.8443	6.7525	324.5472	3.3309
8	6.4999	128.7869	6.5600	332.9684	3.1333
9	6.4999	128.7494	6.3918	340.7592	2.9662
10	6.4999	128.7572	6.1686	351.7627	2.7522

Finally, Fig. 4b shows the coverage path considering $\boldsymbol{\lambda}_6$ solution compared to the solution obtained using the approach proposed by Torres *et al.* [33].

3) Polygon 3 and Polygon 4: For Polygon 3, the solutions generated by the MOEA/D algorithm were largely non-

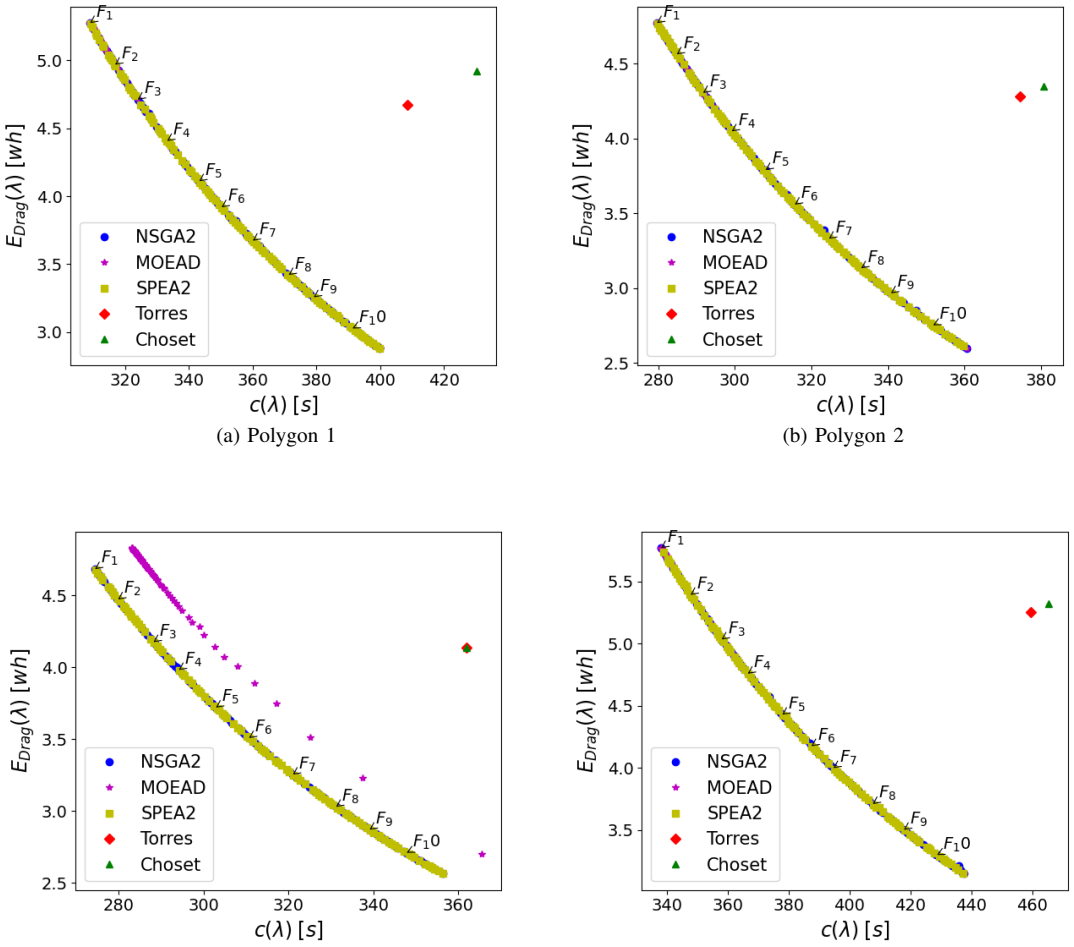

(a) Polygon 1

(b) Polygon 2

(c) Polygon 3

(d) Polygon 4

Fig. 5. Pareto-optimal front for the four case study: comparative analysis of NSGA-II, MOEA/D, and SPEA2.

dominant when compared to the Pareto front produced by NSGA-II (see Fig. 5c). In this case, the NSGA-II solver successfully identified solutions with both lower mission times and lower energy consumption, effectively dominating the MOEA/D set. Fig. 4c shows the coverage path considering $\boldsymbol{\lambda}_6$ solution obtained NSGA-II algorithm.

The polygon 4 represents the most geometrically complex field (concave boundaries with 36 vertices). Despite the increased complexity, NSGA-II and SPEA2 maintained consistent convergence, identifying a diverse range of trade-offs as Fig. 5d presents. The coverage path for polygon 4 is presented in Fig. 4d, obtained with NSGA-II, demonstrating robustness in obtaining coverage paths for agricultural applications.

B. Computational Effort Analysis

The computational effort of the proposed multi-objective optimization framework was evaluated by comparing the performance of three evolutionary algorithms: NSGA-II, MOEA/D, and SPEA2. Each algorithm was configured with a population of 100 individuals and evolved over 100 generations to ensure a fair comparison.

Three metrics were considered to assess the computational efficiency and solution quality: average execution time (AET), Hypervolume (HV), and Spacing (see Table III). The execution times remained consistent across all scenarios, ranging from 28.57 s to 42.36 s. These output times make feasible the framework's use in real-world agricultural applications as an offline planning process.

The performance metrics show that NSGA-II and SPEA2 achieved significantly higher HV values and lower Spacing compared to MOEA/D. Specifically, NSGA-II and SPEA2 produced well-distributed Pareto fronts (Spacing $\approx$ 0.3), whereas MOEA/D exhibited much higher spacing values (above 3.0), indicating a less uniform distribution of trade-offs. MOEA/D exhibited slightly higher computational costs in all polygons, while NSGA-II demonstrated a robust balance between diversity and convergence. These results validate the selection of NSGA-II as the primary solver for the multi-objective optimization problem of the of coverage path planning.

Moreover, each case study was subjected to 30 independent trials to validate the consistency of the optimization results.

TABLE III
COMPARATIVE COMPUTATIONAL EFFORT AND PERFORMANCE OF NSGA-II, MOEA/D AND SPEA2 ALGORITHMS CONSIDERING THE FOURTH POLYGONS

	NSGA-II			MOEA/D			SPEA2		
	AET (s)	HV	Spacing	AET (s)	HV	Spacing	AET (s)	HV	Spacing
1*	33.46	502.10	0.3032	38.76	490.01	3.42	34.36	502.19	0.2326
2	33.48	674.02	0.3079	38.35	664.21	3.02	34.44	671.83	0.2008
3	28.57	699.68	0.2676	32.45	628.21	3.25	28.78	699.51	0.1978
4	37.56	349.08	0.3186	42.36	333.62	3.86	38.20	348.83	0.2848

*Polygon

The low variance observed in the Hypervolume (HV) and Spacing (S) metrics suggests that the NSGA-II solver consistently converges to the Pareto front, ensuring that the performance gains reported over the Choset and Torres benchmarks are representative of the algorithm's steady-state performance rather than isolated stochastic successes.

C. Application to a Spraying Mission - Case study

The multi-objective optimization of Eq. (7), was applied to optimize a real spraying task using the DJI AGRAS T10 drone. This case study aimed to evaluate the practical applicability of the method in an agricultural context.

The target area (see Fig. 6a) corresponds to the area at the Univerdecidade campus of the Federal University of the Triângulo Mineiro (UFTM), Brazil. This area was defined based on high-resolution satellite imagery provided by ESRI [34]. The field boundaries were manually delineated in QGIS, resulting in a rectangular polygon representing the crop area of 1.42 ha. This polygon was then exported as a GeoJSON file and imported into Python using the GeoPandas library for further processing and visualization.

The Pareto-front obtained after solving the multi-objective solution problem for the target area of Fig. 6a is presented in Fig. 6b. Additionally, the solutions considering Choset approach [32] ($\boldsymbol{\lambda} = [5.5\ \text{m} \quad 90\ ^\circ \quad 7\ \text{m/s}]$) and the solution using also the approach proposed by Torres *et al.* [33] was also presented ($\boldsymbol{\lambda} = [5.5\ \text{m} \quad 31.65\ ^\circ \quad 7\ \text{m/s}]$). One can observe that these solutions do not improve the mission time nor the drag energy.

Finally, the coverage path for a spraying mission is presented in Fig. 7a with the obtained design variables that can be used to program the mission in the DJI AGRAS T10 drone ($\boldsymbol{\lambda} = [6.48\ \text{m} \quad 31.32\ ^\circ \quad 6.7\ \text{m/s}]$). Fig. 7b shows the coverage path using the Choset approach [32]. Mainly, the higher velocity using the Choset approach of Fig. 7b implies an increase in energy consumption and also the increment of the mission time (see Fig. 6b).

The practical implementation of the proposed approach involves specific trade-offs over traditional benchmarks. The next subsection explores the advantages and inherent limitations of the proposed methodology in real-world agricultural settings.

D. Advantages and Limitations

The proposed approach offers several advantages. First, it provides a comprehensive framework for mission planning that explicitly integrates the operational requirements of agricultural spraying, ensuring that critical coverage path definitions such as row spacing, sweep direction, and drone velocity are optimized in a unified manner. Second, the approach simultaneously minimizes both mission time and energy consumption by formulating the problem as a multi-objective optimization, thereby improving the efficiency and sustainability of spraying operations. Third, the framework is validated through a real case study using the DJI AGRAS T10 drone, demonstrating its practical applicability and superiority over conventional coverage path strategies.

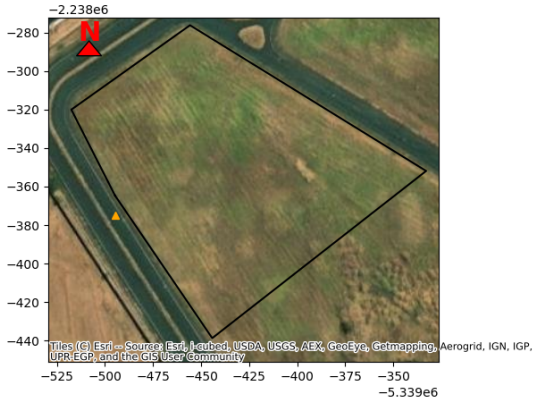

(a) Targe area

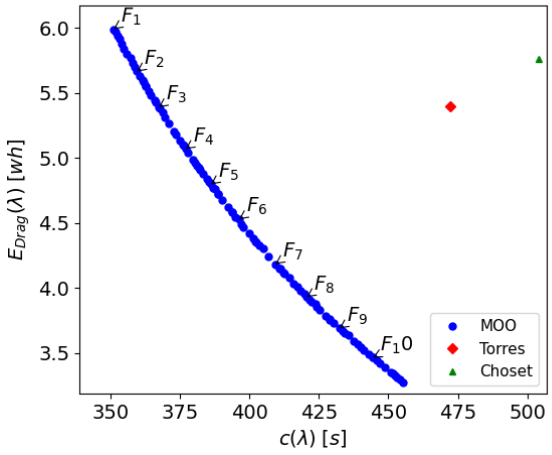

(b) Pareto Front

Fig. 6. Case study: (a) Geographic representation of the target field area with optimized trajectory overlay; (b) Corresponding Pareto-optimal front showing the trade-off between mission time and energy consumption.

Nonetheless, the proposed method has the following limitations:

1) At this stage, the framework applies only to convex polygonal fields, thereby excluding irregular or concave fields that commonly define real agricultural target areas.
2) The framework does not account for static or dynamic obstacles within the area of interest, limiting its applicability in scenarios involving trees, poles, or other

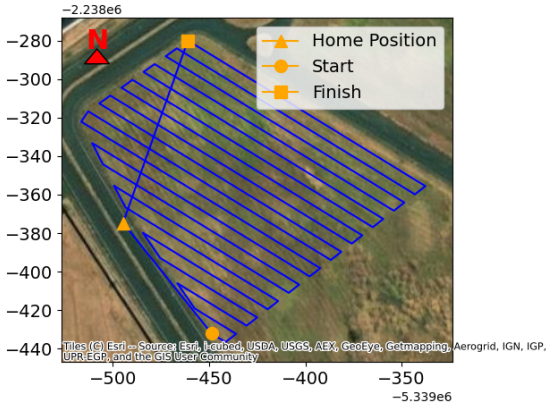

(a) CP with MOO ($\boldsymbol{\lambda}_6$)

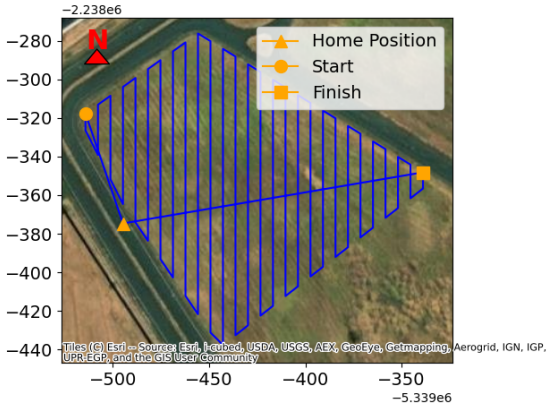

(b) CP using Choset approach [32]

Fig. 7. Comparison of mission trajectories: (a) Time-optimal path, prioritized from the multi-objective approach; (b) Path obtained with Choset approach [32].

infrastructure elements.

3) No spraying operational performance, such as pesticide drift, application uniformity, or overlap precision, was not included in the optimization framework.

Future developments should focus on extending the approach to non-convex fields and incorporating obstacle-avoidance strategies, aiming to enhance its robustness and practical relevance.

IV. Conclusions

This work presented a multiobjective optimization framework for mission planning of agricultural spraying drones to enhance the efficiency of coverage path planning. The proposed approach optimizes row spacing, sweep direction, and drone velocity, addressing the dual objectives of minimizing energy consumption and total mission duration.

The case study conducted with the DJI AGRAS T10 drone demonstrated the practical applicability of the method. The optimized coverage paths provided by the proposed framework resulted in improved energy efficiency and shorter mission times compared to conventional strategies. Importantly, the approach integrates realistic operational requirements of spraying missions, making it directly relevant for precision agriculture practices.

Finally, it is worth mentioning that the solution to the multiobjective problem yields a set of optimal solutions, referred to as the Pareto front. The designer should evaluate the optimal solutions to determine a specific solution that can be programmed into the agricultural drone. Consequently, the resulting set of optimal solutions represents a potential advantage in optimizing the coverage path, as the designer can select a single coverage path from the set of optimal coverage paths, allowing for weighing the energy consumption or mission time of the agricultural drone with flexibility.

The findings reveal that traditional methods for agricultural spraying, based on simple geometric heuristics, result in an energy penalty. Energy consumption can be reduced by 14.2% without a proportional increase in mission time by shifting to a multi-objective Pareto-based framework. These highlight that the optimal path corresponds not only to a single solution but a spectrum of choices that depend on the specific battery health and operational window of the UAV. Thus, these optimal paths can be applied to agricultural tasks.

The present research study is based on a multi-objective framework that considers the critical trade-off between mission time and energy consumption. Future iterations could incorporate additional conflicting objectives, such as minimizing pesticide drift, application uniformity, overlap precision or optimizing for the remaining chemical volume in the spray tank. Future research will integrate Digital Elevation Models (DEM) to adjust the row spacing dynamically based on the slope of the terrain, as well as validating the approach in large-scale field experiments.

Acknowledgments

This research was supported by the Universidade Federal do Triângulo Mineiro (UFTM). No additional external funding was received for this study. Fran S. Lobato thanks the Brazilian agency CNPq for the financial support through the granting of a research scholarship (Process n° 309178/2023-1).

Appendix A
Torres *et al.* [33] approach for CP

Algorithm 1 Line Sweep Direction Algorithm

Input: Polygon with n vertices
Output: Optimal sweep angle θ
for each polygon edge **do**
    Compute the edge normal direction
    Measure the maximum distance of all vertices to this edge
    if this distance is smaller than the current minimum **then**
        Update the optimal direction
    end if
end for
Compute θ as the angle of the optimal direction
Return θ

REFERENCES

[1] S. Qazi, B. A. Khawaja, and Q. U. Farooq, "Iot-equipped and ai-enabled next generation smart agriculture: A critical review, current challenges and future trends," *Ieee Access*, vol. 10, pp. 21 219–21 235, 2022, doi:10.1109/ACCESS.2022.3152544.

[2] L. F. Oliveira, A. P. Moreira, and M. F. Silva, "Advances in agriculture robotics: A state-of-the-art review and challenges ahead," *Robotics*, vol. 10, no. 2, p. 52, 2021, doi:10.3390/robotics10020052.

[3] R. Guebsi, S. Mami, and K. Chokmani, "Drones in precision agriculture: A comprehensive review of applications, technologies, and challenges," *Drones*, vol. 8, no. 11, p. 686, 2024, doi:10.3390/drones8110686.

[4] A. Hafeez, M. A. Husain, S. Singh, A. Chauhan, M. T. Khan, N. Kumar, A. Chauhan, and S. Soni, "Implementation of drone technology for farm monitoring & pesticide spraying: A review," *Information processing in Agriculture*, vol. 10, no. 2, pp. 192–203, 2023, doi:10.1016/j.inpa.2022.02.002.

[5] U. R. Mogili and B. Deepak, "Review on application of drone systems in precision agriculture," *Procedia computer science*, vol. 133, pp. 502–509, 2018, doi:10.1016/j.procs.2018.07.063.

[6] C. Di Franco and G. Buttazzo, "Coverage path planning for uavs photogrammetry with energy and resolution constraints," *Journal of Intelligent & Robotic Systems*, vol. 83, no. 3, pp. 445–462, 2016, doi:10.1007/s10846-016-0348-x.

[7] F. A. Lara-Molina, "Optimization of coverage path planning for agricultural drones in weed-infested fields using semantic segmentation," *Agriculture*, vol. 15, no. 12, p. 1262, 2025, doi:10.3390/agriculture15121262.

[8] T. M. Cabreira, L. B. Brisolara, and F. J. Paulo R, "Survey on coverage path planning with unmanned aerial vehicles," *Drones*, vol. 3, no. 1, p. 4, 2019, doi:10.3390/drones3010004.

[9] L. Bostelmann-Arp, C. Steup, and S. Mostaghim, "Multi-objective seed curve optimization for coverage path planning in precision farming," in *Proceedings of the Genetic and Evolutionary Computation Conference*, 2023, pp. 1312–1320, doi:10.1145/3583131.3590490.

[10] H. Tian, Z. Mo, C. Ma, J. Xiao, R. Jia, Y. Lan, and Y. Zhang, "Design and validation of a multi-objective waypoint planning algorithm for uav spraying in orchards based on improved ant colony algorithm," *Frontiers in Plant Science*, vol. 14, p. 1101828, 2023, doi:10.3389/fpls.2023.1101828.

[11] K. O. Ellefsen, H. A. Lepikson, and J. C. Albiez, "Planning inspection paths through evolutionary multi-objective optimization," in *Proceedings of the Genetic and Evolutionary Computation Conference 2016*, 2016, pp. 893–900, doi:10.1145/2908812.2908883.

[12] L. Bostelmann-Arp, C. Steup, and S. Mostaghim, "Free-form coverage path planning of quadcopter swarms for search and rescue missions using multi-objective optimization," in *2024 IEEE Congress on Evolutionary Computation (CEC)*. IEEE, 2024, pp. 1–8, doi:10.1109/CEC60901.2024.10611984.

[13] K. O. Ellefsen, H. A. Lepikson, and J. C. Albiez, "Multiobjective coverage path planning: Enabling automated inspection of complex, real-world structures," *Applied Soft Computing*, vol. 61, pp. 264–282, 2017, doi:10.1016/j.asoc.2017.07.051.

[14] U. Orozco-Rosas, K. Picos, and O. Montiel, "Hybrid path planning algorithm based on membrane pseudo-bacterial potential field for autonomous mobile robots," *IEEE Access*, vol. 7, pp. 156 787–156 803, 2019, doi:10.1109/ACCESS.2019.2949835.

[15] U. Orozco-Rosas, O. Montiel, and R. Sepúlveda, "Mobile robot path planning using membrane evolutionary artificial potential field," *Applied soft computing*, vol. 77, pp. 236–251, 2019, doi:10.1016/j.asoc.2019.01.036.

[16] U. Orozco-Rosas, K. Picos, J. J. Pantrigo, A. S. Montemayor, and A. Cuesta-Infante, "Mobile robot path planning using a qapf learning algorithm for known and unknown environments," *IEEE Access*, vol. 10, pp. 84 648–84 663, 2022, doi:10.1109/ACCESS.2022.3197628.

[17] X. Xu, C. Xie, Z. Luo, C. Zhang, and T. Zhang, "A multi-objective evolutionary algorithm based on dimension exploration and discrepancy evolution for uav path planning problem," *Information Sciences*, vol. 657, p. 119977, 2024, doi:10.1016/j.ins.2023.119977.

[18] X. Liu, L. Gao, Z. Guan, Y. Song, and R. Zhang, "A multi-objective optimization model for planning unmanned aerial vehicle cruise route," *International Journal of Advanced Robotic Systems*, vol. 13, no. 3, p. 116, 2016, doi:10.5772/64165.

[19] X. Zhang, S. Xia, X. Li, and T. Zhang, "Multi-objective particle swarm optimization with multi-mode collaboration based on reinforcement learning for path planning of unmanned air vehicles," *Knowledge-Based Systems*, vol. 250, p. 109075, 2022, doi:10.1016/j.knosys.2022.109075.

[20] V. Ajith and K. Jolly, "Hybrid optimization based multi-objective path planning framework for unmanned aerial vehicles," *Cybernetics and Systems*, vol. 54, no. 8, pp. 1397–1423, 2023, doi:10.1080/01969722.2022.2157607.

[21] X. Zhen, Z. Enze, and C. Qingwei, "Rotary unmanned aerial vehicles path planning in rough terrain based on multi-objective particle swarm optimization," *Journal of Systems Engineering and Electronics*, vol. 31, no. 1, pp. 130–141, 2020, doi:10.21629/JSEE.2020.01.14.

[22] H. Bai, T. Fan, Y. Niu, and Z. Cui, "Multi-uav cooperative trajectory planning based on many-objective evolutionary algorithm," *Complex System Modeling and Simulation*, vol. 2, no. 2, pp. 130–141, 2022, doi:10.23919/CSMS.2022.0006.

[23] M. K. Singh, A. Choudhary, S. Gulia, and A. Verma, "Multi-objective nsga-ii optimization framework for uav path planning in an uav-assisted wsn," *The Journal of Supercomputing*, vol. 79, no. 1, pp. 832–866, 2023, doi:10.1007/s11227-022-04701-2.

[24] Q. Zhang and H. Li, "Moea/d: A multiobjective evolutionary algorithm based on decomposition," *IEEE Transactions on Evolutionary Computation*, vol. 11, no. 6, pp. 712–731, 2007, doi:10.1109/TEVC.2007.892759.

[25] E. Zitzler, M. Laumanns, and L. Thiele, "Spea2: Improving the strength pareto evolutionary algorithm," *Evolutionary Methods for Design, Optimisation and Control with Application to Industrial Problems*, pp. 95–100, 2001.

[26] J. E. Silva, W. H. B. da Silva, M. A. J. Ferraz, E. A. S. Menezes, O. P. da Costa, F. D. Inácio, T. O. C. Barboza, C. A. D. Melo, G. R. Carvalho, and A. F. dos Santos, "Impact of spray volume and flight speed on the efficiency of drone applications in coffee plants of different ages," *Smart Agricultural Technology*, vol. 9, p. 100694, 2024, doi:10.1016/j.atech.2024.100694.

[27] A. Thibbotuwawa, P. Nielsen, B. Zbigniew, and G. Bocewicz, "Energy consumption in unmanned aerial vehicles: A review of energy consumption models and their relation to the uav routing," in *International Conference on Information Systems Architecture and Technology*. Springer, 2018, pp. 173–184, doi:10.1007/978-3-319-99996-8_16.

[28] V. R. Bolzon and F. A. Lara-Molina, "Optimal kinematic and elastodynamic design of planar parallel robot with flexible joints," *IEEE Latin America Transactions*, vol. 16, no. 5, pp. 1343–1352, 2018, doi:10.1109/TLA.2018.8408426.

[29] F. A. Lara-Molina, D. Dumur, and K. Assolari Takano, "Multi-objective optimal design of flexible-joint parallel robot," *Engineering Computations*, vol. 35, no. 8, pp. 2775–2801, 2018, doi:10.1108/EC-01-2018-0015.

[30] F. R. Moreira, F. S. Lobato, A. A. Cavalini Jr, and V. Steffen Jr, "Robust multi-objective optimization applied to engineering systems design," *Latin American Journal of Solids and Structures*, vol. 13, no. 9, pp. 1802–1822, 2016, doi:10.1590/1679-78252801.

[31] F. S. Lobato and V. Steffen Jr, *Multi-objective optimization problems: concepts and self-adaptive parameters with mathematical and engineering applications*. Springer, 2017, doi:10.1007/978-3-319-58565-9.

[32] H. Choset and P. Pignon, "Coverage path planning: The boustrophedon cellular decomposition," in *Field and service robotics*. Springer, 1998, pp. 203–209, doi:10.1007/978-1-4471-1273-0_32.

[33] M. Torres, D. A. Pelta, J. L. Verdegay, and J. C. Torres, "Coverage path planning with unmanned aerial vehicles for 3d terrain reconstruction," *Expert systems with applications*, vol. 55, pp. 441–451, 2016, doi:10.1016/j.eswa.2016.02.007.

[34] Esri, Impact Observatory, and Microsoft, "Esri 10-meter land use/land cover (lulc) map," https://livingatlas.arcgis.com/landcover/, 2021, accessed: August 6, 2025.

Fabian Andres Lara-Molina Mechatronics Engineer, 2005 from the Universidad Militar Nueva Granada. Master's and PhD in Mechanical Engineering from the State University of Campinas, 2008 and 2012, respectively. Currently, he is associate professor in the Department of Mechanical Engineering at the Federal University of Triângulo Mineiro, Uberaba-MG,Brazil. He has experience in the field of Mechanical Engineering, mainly working in dynamics and control of mechanical systems.

Fran Sérgio Lobato received his degree in Chemical Engineering, a Master of Science in Chemical Engineering, and a Doctorate in Mechanical Engineering from the Federal University of Uberlândia, Brazil, in 2001, 2004, and 2008, respectively. In 2009, he worked at the Federal University of São João del-Rei, Brazil. Since 2010, he has been a professor at the School of Chemical Engineering, Federal University of Uberlândia. His current research interests include bio-inspired optimization algorithms, optimal control theory, uncertainty analysis, heat transfer problems, and the formulation and solution of inverse problems.

Maicon Fábio Appelt Agronomy, 2012 from the Federal University of Viçosa. Master in vegetal production from the Federal University of Viçosa, 2014. Currently, he is research engineering at Fertirriga, Rio Paranaíba-MG, Brazil. Has experience in the field of pastures, forage production, soil fertility and water resources, with an emphasis on fertigation.